A Letters Journal Exploring the Frontiers of Physics

December 2014

EPL, **108** (2014) 56001 www.epljournal.org
doi: 10.1209/0295-5075/108/56001

Rigidity transitions in glasses driven by changes in network dimensionality and structural groupings

K. Vignarooban[1(a)], P. Boolchand[1], M. Micoulaut[2], M. Malki[3,4] and W. J. Bresser[5]

[1] *School of Electronics and Computing Systems, College of Engineering and Applied Science, University of Cincinnati Cincinnati, OH 45221-0030, USA*
[2] *Laboratoire de Physique Théorique de la Matière Condensée Université Pierre et Marie Curie Boite 121, 4, Place Jussieu, 75252 Paris Cedex 05, France*
[3] *CEMHTI, CNRS UPR 3079 - 1D, Avenue de la Recherche Scientifique, 45071 Orleáns Cedex 02, France*
[4] *Université d'Orléans (Polytech Orléans) - BP 6749, 45072 Orléans Cedex 02, France*
[5] *Physics and Geology Department, Northern Kentucky University - Highland Heights, KY 41099, USA*

received 2 September 2014; accepted 6 November 2014
published online 26 November 2014

PACS 61.43.Fs – Structure of solids and liquids; crystallography: Glasses
PACS 64.70.pm – Glass transitions of specific systems: Liquids
PACS 63.50.Lm – Vibrational states in disordered systems: Glasses and amorphous solids

Abstract – Calorimetric, Raman and electrical conductivity properties of alkali borates $(100-x)B_2O_3$-xM_2O (M = Li, Na) are studied as a function of composition (x) and these show the presence of stiffness transitions and an intermediate phase which are driven by a combination of network dimensionality change and usual topological constraint changes. This picture is confirmed by a detailed Raman analysis showing that specific modes of molecular structural groupings dominate the network structure in the intermediate phase. Their evolution shows a one-to-one correspondance with the observed non-reversing heat flow at the glass transition, and are correlated with thresholds in ionic conductivity that allows identifying a flexible phase at high alkali content, whereas the mildly stressed-rigid B_2O_3-rich glasses are driven by the conversion of planar 2D boroxol ring structures into the 3D structural groupings. These findings deeply modify the usual picture of these archetypal glasses, and reveal the very first example of the onset of rigidity tuned by network dimensional conversion.

Rigidity theory provides a remarkably powerful atomic scale approach to understanding the effect of composition on physical, chemical and mechanical properties of disordered solids [1]. It has received renewed attention in recent years due, in part, to promising and quite unexpected applications in materials science and technology [2–4]. While the core of the theory relies essentially on the early work of Maxwell [5] on mechanical constraints and rigidity of macroscopic structures, its application to amorphous covalent networks has emerged from the recognition that bond-stretching (BS) and bond-bending (BB) interatomic interactions can be treated in the same way [6]. Specifically, the number of constraints n_c arising from such forces are compared to the dimensionality D of the space in which the atomic structure is embedded. When $n_c = D$, one recovers the usual Maxwell stability criterion of isostatic structures and, in glasses, this particular condition has been identified with a rigidity transition [7,8] separating weakly connected flexible (or hypostatic) from stressed-rigid (hyperstatic) networks having a large connectivity. At the transition point, the number of low-frequency (floppy) modes $\mathcal{F} = D - n_c$ found in the flexible phase vanish [9], and act as an order parameter. There has been a vast body of experimental literature [10] showing that such elastic phase transitions can be detected from calorimetric, optical, or mechanical probes in chalcogenide and oxide glasses.

In most of these materials, the network is considered to be three-dimensional, $D = 3$, so that the number of constraints n_c is essentially changed by an appropriate alloying of a chain cross-linker in order to achieve the transition $n_c = D$. While several theoretical studies of rigidity transitions have focused on simple 2D lattices [11,12],

[(a)] Present address: Department of Physics, Faculty of Science, University of Jaffna - Jaffna 40000, Sri Lanka.

corresponding experimental studies have not been considered so far, because there are actually only a limited number of glassy materials showing a local 2D dimension. Such a situation is met in alkali borates $(100-x)B_2O_3$-xM_2O (M = Li, Na) which are, among the oxide glasses, unusual in many respects. Indeed, the base oxide, B_2O_3, is composed of planar (2D) BO_3 triangles (B3), with a majority (> 75% [13,14]) of these local units forming part of 3-membered planar rings —boroxyl rings (BR)— which comprise elements of medium-range structure. Lithia or soda alloying leads to the replacement of B3 by a tetrahedrally coordinated boron (B4) with a charge compensating alkali [15], and furthermore involves changes leading to the formation of 3D "*mixed rings*" composed of various ratios of B3:B4 species (from 3:0 (BR) up to 1:2 in disodium triborate) in structural groupings (SG) identified as pentaborate, tetraborate or triborate medium-range structures, as revealed from systematic ^{11}B NMR [16], Raman scattering [17], Infrared reflectance studies [18] as a function of alkali content. These networks, thus, obviously evolve from a 2D to a 3D *local* structure.

In this letter we report, for the first time, on the existence of rigidity transitions driven by changes in network dimensionality. Our analysis shows that three elastic phases —stressed-rigid, intermediate, flexible— actually emerge when *both* the local dimension and the connectivity (or n_c) of the network backbone of alkali borates $(100-x)B_2O_3$-xM_2O with M = Li (LiB, hereafter) and M = Na (NaB) are tuned as a function of alkali content. Local structures and medium-range superstructures (structural groupings, SG) form with alkali alloying, and are characterized at a level of unprecedented accuracy. At low alkali content ($x < 20\%$) *pure* (BR) *rings* convert to *mixed rings* as the network global connectivity increases with increasing alkali content, as reflected in the glass transition temperature T_g variation. However, the Raman active symmetric stretch frequency of the BR steadily softens and broadens suggesting a steady increase of network dimensionality from quasi-2D at $x = 0$ to 3D at $x \simeq 20\%$. In the present glasses the increase of network connectivity comes at the expense of a dimensionality increase, as B4 units replace B3 ones leading to global softening of the backbone. That view of a dimensional regression is independently supported from the boson mode scattering strength and the dc ionic conductivity variation with alkali content as we discuss here.

To provide a general framework for the experimental investigations, particularly compositional studies, we first use a mean-field model of topological constraint counting [19] in 2D and 3D, in combination with a simple relationship between connectivity and subnetwork dimensionality of amorphous alloys [20]. In order to explore the Maxwell stability criterion of alkali borates, and to balance the constraint count n_c with the change in D, we first calculate structural correlations in a (B3,B4) network structure with respective concentrations N_3 and N_4. Assuming that there are no B4-B4 connections at low alkali content,

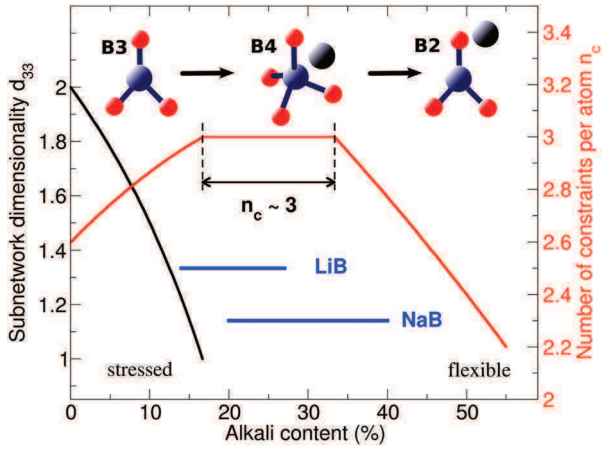

Fig. 1: (Color online) Top: typical local structures found in alkali borates: a $BO_{3/2}$ triangle (B3), a $MBO_{4/2}$ tetrahedron (B4), and $MBO_{3/2}$ triangle containing one non-bridging oxygen (B2). Bottom: behavior of the 3-3 subnetwork dimensionality d_{33} in $(100-x)B_2O_3$-xM_2O as a function of alkali content x. Right axis: calculated number of topological constraints n_c as a function alkali content x (eq. (2), red curve). The isostatic compositional intervals for Li- and Na-borates (LiB and NaB) are determined from fig. 2.

the statistical distribution of pairs N_{ij} $(i,j = 3,4)$ [16], and the partial coordination numbers $C_{ij} = N_{ij}/N_i$ can be calculated:

$$C_{33} = \frac{3-10x}{1-2x}, \qquad C_{34} = \frac{4x}{1-2x} \tag{1}$$

and, of course, $C_{44} = 0$ and $C_{43} = 4$ when x is low (< 0.20). In eq. (1), x is written as mole fraction of modifier. We then build on the approach of Mosseri and Dixmier [20] by defining a dimensionality $d_{ij} = C_{ij} - 1$ of *local* arrangements of bonds around a given unit, B3 or B4. When the partial coordination number is three (*i.e.* $C_{33} = 3$ met at $x = 0$), then the dimensionality takes an integer value, and the dimension of the associated subnetwork is 2. For the 33 network (B_2O_3-like), one has from eq. (1): $d_{33} = (2-8x)/(1-2x)$ which decreases $(1 < d_{ij} < 2)$ as a function of alkali content x, and becomes filamentary, *i.e.* $d_{33} \simeq 1$ as x approaches $x_c \simeq 1/6$. When the dimensionality of this subnetwork becomes less than 1 ($x > x_c = 16.6\%$), this B3 subnetwork now consists of isolated regions of B3-B3 connections. One can, therefore, consider that for compositions fulfilling $x > x_c$, the whole network has now become fully 3D (black curve in fig. 1).

To calculate the number of constraints n_c, we first use the random pair model of Gupta [15,21] which gives the statistics p_i (i = B3, B4 and B2) of local structures as a function of alkali content. At low content, conservation of charge leads immediately to $p_{B4} = x/(1-x)$ and $p_{B3} = 1 - p_{B4}$ as the presence of B2 units can be safely neglected up

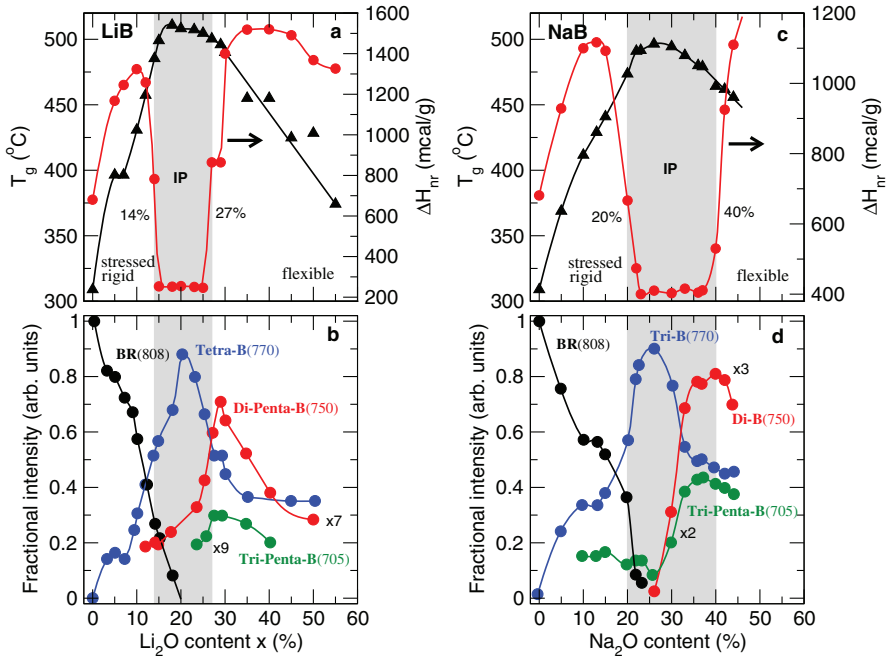

Fig. 2: (Color online) Glass transition T_g (a), non-reversing heat flow ΔH_{nr} ((a), red curve, right axis) and Raman mode scattering strength variation due to mixed rings (b) as a function of lithium content x in $(100-x)B_2O_3$-xLi_2O (LiB) glasses. Glass transition T_g (c), non-reversing heat flow ΔH_{nr} ((c), red curve, right axis) and Raman mode scattering strength variation due to mixed rings (d) as a function of sodium content x in $(100-x)B_2O_3$-xNa_2O (NaB) glasses. In both glasses, the deep square-well defined minimum of ΔH_{nr} defines an intermediate phase (IP, gray zone) between the stressed-rigid and the flexible phase. As shown in (b) pentaborates (PB: 16.6%) and tetraborates (Tetra-B: 20%) determine the IP width in LiB, while in (d) tetraborates (Tetra-B: 20%) and triborates (Tri-B: 25%), and to a lesser extent diborates (Di-B: 33.3%) and tripentaborates (Tri-Penta-B: 37%) species are responsible for the IP in Na-B.

to $x \simeq 33.3\%$. At higher compositions ($x > 33.33\%$), the presence of B2 units leads to the depolymerization of the network structure, and a reduction of network connectivity as reflected in the glass transition temperature variation (see below). We then enumerate constraints [19] of the system using

$$n_c(x) = \frac{\sum_i N_c^i p_i(x)}{\sum_i \mathcal{N}^i p_i(x)}, \qquad (2)$$

where N_c^i is the number of constraints of species i (i = B3,B4,B2) computed in 2D ($x < x_c$) or 3D ($x > x_c$) for B3, and in 3D for the other species, and $\mathcal{N}^i$ is the number of atoms of species i. The evolution of n_c with alkali content is shown in fig. 1 (red curve), and the conclusion becomes apparent when $n_c(x)$ is compared with the evolution of $D(x)$. In the base network (B_2O_3), the *local* dimension of the network is 2D and the network is stressed rigid ($\mathcal{F}(0) = D - n_c(0) = -0.6$). As the alkali content x is increased, B3 units convert into B4 ones, which accomodate charge compensation, and result in an increase of n_c (eq. (2)). However, at the same time, the dimensionality d_{33} of the B3 subnetwork decreases, and a 3D network driven by B3-B4 correlations sets in, reducing the number of floppy modes $\mathcal{F} = D(x) - n_c(x)$. At $x_c = 16.66\%$, the network can be viewed as 3D, and the Maxwell stability criterion $n_c \simeq 3$ is achieved by a simultaneous increase of $D(x)$ and $n_c(x)$. We are not aware of any other system where such combined effects take place. The presence of a finite width Δx where the network can be viewed as isostatically rigid indicates the possibility of the formation of a stress-free intermediate phase (IP) [10,19,22].

In order to detect the latter, we have performed MDSC experiments and established the compositional variation in the $T_g(x)$ and enthalpy of relaxation $\Delta H_{nr}(x)$ at T_g of LiB and NaB glasses[1]. The minuscule $\Delta H_{nr}(x)$ term (red curves in fig. 2(a), (c)) in compositional reversibility windows ($14\% < x < 27\%$ and $20\% < x < 40\%$ for LiB and NaB, respectively) is the signature for the isostaticity of that phase, as previously established for a large number of inorganic glasses [10,22,23]. For the case of NaB, we furthermore detect that the centroid ($\simeq 30\%$) of our IP is related to the compositional location of a fragility anomaly in the corresponding liquid [15], a correlation also established recently [23]. We identify it with the rigid but unstressed nature of networks occurring in that composition range, *i.e.*, representing the IP (fig. 1). The compositional trends in glass transition temperature in LiB and NaB interestingly show a maximum of $T_g(x)$ that is located nearly in the center of the reversibility window. The

[1]See synthesis and characterization in the supplementary information available at `http://secs.ceas.uc.edu/~pboolcha/journals.htm`.

Table 1: Left: identified Raman mode frequency f (in cm^{-1}), composition x_p at which corresponding fractional intensity is maximized (fig. 2(b), (d)); right: nature of the structural grouping (SG), and corresponding B3:B4 ratio and stoichiometry x_{SG}.

f (cm^{-1})	Glass	x_p(%)	Structural grouping	B3:B4	x_{SG}(%)
808	B_2O_3	0	BR	3:0	0
			Penta-B	4:1	16.7
770	LiB	20.0	Tetra-B	3:1	20.0
770	NaB	26.0	Tri-B	2:1	25.0
750	LiB	29.0	Di-Penta-B	3:2	28.5
740	NaB	38.0	Di-B	1:1	33.3
705	LiB	30.0	Tri-Penta-B	2:3	37.5
705	NaB	37.0			
			Di-Tri-B	1:2	40.0

observation suggests the minimal role of non-bridging oxygen to aspects of structure that determine the reversibility window given that B2 onsets only at $x > 33.33\%$ [15,21]. But unlike all the previous cases investigated [10,22,23], in the present case of alkali borates one is able to establish the non-random nature of structural groupings (SG) that contribute to the formation of the IP. This is obtained from detailed Raman scattering results.

The present conclusions (fig. 2(b), (d)) first build on the assignment of Brill [24], who recognized that alloying Na_2O into a B_2O_3 base glass leads to a conversion of BR (with B3 to B4 ratio 3:0) into a mixed ring (MR) having two B3 and one B4 (2:1) with a compensating Na cation in its vicinity. The vibrational signature of these ring species are well recognized: the $808\,cm^{-1}$ mode for BR [13,25], and the $770\,cm^{-1}$ mode for a MR. Vibrational modes of these ring species are observed in Raman scattering (see supplementary information available at the web site given in footnote [1]). It has also been recognized [24] that the red-shift ($770\,cm^{-1}$) of the MR compared to the BR-mode ($808\,cm^{-1}$) is due to the longer length of an sp^3 tetrahedral bond (1.43 Å) compared to a planar sp^2 one (1.32 Å) as replacement of a B3 by a B4 lowers the effective spring constant of the ring resulting in the red-shift of the symmetric stretch vibration.

Other typical structural groupings (SG) containing mixed ring species [16] include pentaborate (Penta-B), triborate (Tri-B) and tetraborate (Tetra-B), which correspond to a well-defined stoichiometry x_{SG} (table 1). Once the Raman spectra are deconvoluted and their parameters determined (frequency f, linewidth, intensity) and followed with alkali content, non-monotonic behaviors (fig. 2(c), (d)) are found for certain modes, and these display maxima in the fractional integrated intensity at various compositions x_p (fig. 2(b), (d) and table 1). These observed composition maxima x_p are then compared to those (x_{SG}) which are associated with SGs given that one expects their corresponding mode scattering strength to show maxima as well. For instance, stoichiometry imposes that for an alkali Tetra-B the maximum in mode scattering should occur near $x_{GS} = 20\%$, and near 16.6% for an alkali Penta-B. This allows decoding the nature of the SGs (table 1) found by tracking Raman mode scattering strenghts. More importantly, we arrive at the conclusion that select structural groupings populate the IP compositions, and their evolution with alkali content x can be associated with the boundaries of the IP.

As seen from fig. 2(b), with the smaller-sized alkali-ion, Li-Penta-B and Li-Tetra-B contribute to the formation of the IP. On the other hand, with the larger-sized alkali-ion, sodium Tri-B groupings are dominant, while diborate (Di-B) and Tri-Penta-B groupings contribute to a lesser extent to the IP. Note that in going from Li to Na, the IP centroid shifts to higher x and also becomes wider in x. These trends are manifestations of the higher crystal field of the smaller Li^+-ion compared to the Na^+ ion that stabilizes the higher multiborate groupings (Penta- and Tetra-) with the former than with the latter. The multi-borate groupings house the B4 cations, and remarkably the features of the calorimetric data that maximizes T_g, Raman scattering results also maximize select multi-borate SGs. A constraint count on these structural groupings shows that these have $n_c \simeq 3$, and will lead to networks that display the usual signatures of isostaticity such as space filling tendencies [26] or thermal expansion anomalies [27].

Finally, we present dc conductivity σ on LiB and NaB glasses as a function of composition (fig. 3). Interestingly, we find that σ tracks the transition from a stressed-rigid to isostatic network, given that the IP boundaries ($x = 14\%$ and 20% for LiB and NaB, respectively) are manifested by striking jumps in ionic conduction as previously discovered in other solid electrolytes [28,29], and established from an ion hopping model [30]. It should be noted that the activation energy E_A which is calculated from the Arrhenius temperature behavior of $\sigma(T)$, also displays an important jump near 14% and 20% for LiB and NaB, respectively (see supplementary information available at the web site given in footnote [1]). At very low compositions ($x < 14\%$), both LiB and NaB systems behave similarly, and display a moderate increase of $\sigma(x)$. But, as glasses soften, a rather striking increase of σ by several orders of magnitude for moderate changes in alkali content is observed,

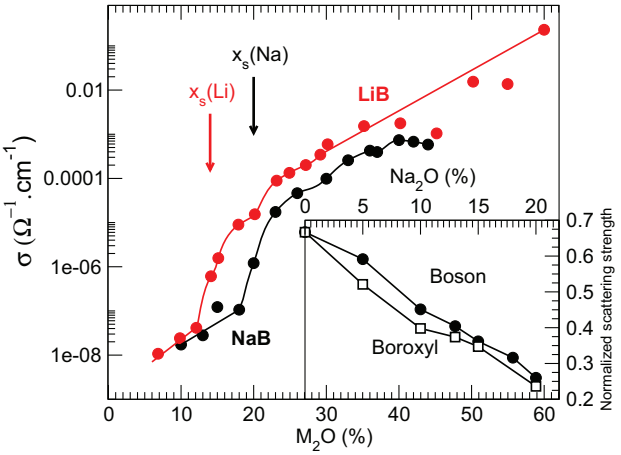

Fig. 3: (Color online) dc ionic conductivity at 300 °C in lithium (red dots) and sodium (black dots) borate glasses as a function of modifier content x at 300 °C. The inset shows the Boson mode scattering strength variation.

and it underscores the loss of stressed rigidity induced by these dimensional changes. Ultimately, flexible network backbones ($x > 40\%$) emerge, which more easily elastically deform due to presence of floppy modes, resulting in an enhanced ion diffusion.

The physical picture that emerges from our results is as follows. The locally 2D character of sp^2 bonded 3-fold B in the base B_2O_3 glass, experiments supported by rigidity theory, shows that when the base glass is modified by alkali oxide (Li_2O or Na_2O), physical properties including calorimetric, Raman scattering and ionic conductivity evolve compositionally to display the fingerprints of a stress-elastic phase transition that is driven by an underlying network dimensional regression. The nature of the isostatically rigid SGs that contribute to the IP is identified by detailed Raman mode frequency and scattering strength variation in dry and homogeneous glasses. These results confirm that the crystal field effect of $Li^{\oplus}$ higher than that of the $Na^{\oplus}$ ion underlies their formation. In addition, the Raman data also show the boson mode scattering strength to be the highest in the base glass (B_2O_3), and to steadily decrease scaling linearly with the BR mode scattering strength (inset of fig. 3), and to nearly vanish as the soda content increases to about $x = 20\%$ (fig. 2(d)). The boson mode, viewed as a floppy mode [31,32] in a network glass, would then clearly be inconsistent with a model of the present glasses consisting of an isostatic base glass (B_2O_3) that steadily softens upon soda alloying. On the other hand, our observation is fully consistent with the much weaker off planar van der Waals interactions serving to stabilize the locally 2D BRs (with respect to the much stronger intra-planar interactions) embedded in a 3D network. The boson mode is, indeed, viewed as a low-frequency defect mode [33] with its high intensity in the stressed-rigid base glass (B_2O_3) reflecting the high BR fraction, and its intensity vanishing as the BR-fraction vanishes upon soda alloying. It is believed that these effects are generic, and given the commonality of findings between LiB and NaB, should certainly be observable in other families of borates (potassium or alkaline-earth based), while also extendable to multicomponent glasses having borates as a base ingredient.

The present work reports the first experimental realization of flexible to rigid transitions driven by dimensional crossover, close to what has been reported theoretically in purely 2D networks [11,34]. Our results emphasize the central role played by local dimensional changes upon alloying, and highlight the presence of certain isostatic SGs which maximize in the intermediate phase. The relationship between superstructures and rigidity transitions has rarely been addressed in the literature, except for the single case of Ge-Se glasses where tetrahedral edge-sharing structures were viewed to drive the IP [19], in spite of a lack of convincing signatures from experiment [8]. The well-defined spectroscopic signature of these SGs in Raman scattering reveals intermediate-range structures to be deeply connected to the stress-free IP. The anomalous behavior of structure with composition should be detected in diffraction experiments. Recent results from Molecular Dynamics simulations [35] seem to give support to this idea.

Borates are widely used in industrial applications [2,36,37]. Our results of a flexible to rigid transition in two of the most common borate glasses (LiB and NaB), leads to the perspective that the elastic properties of such glasses can be used to optimize specific functionalities including network stability, stress-free character and weak aging (an IP property [10]), soft networks promoting ionic conduction (a flexible phase property) for applications in solid-state batteries. It is quite unexpected, and indeed remarkable that these spectacular changes in physical properties are driven by local dimensional changes and the breakdown of the local 2D boroxyl rings. The present approach differs from the coarse graining approach [38] in that the role of modifiers and the dimensional regression explicitely considered in enumerating constraints and leads in a natural fashion to the IP.

* * *

It is a pleasure to acknowledge discussions with Dr. J. Mauro, Prof. R. Kerner and Prof. J. C. Phillips. This work is supported by NSF for grant DMR 08-53957 to University of Cincinnati. M. Micoulaut acknowledges the Franco-American Fulbright Fellowship, and International Materials Institute for support.

REFERENCES

[1] Thorpe M. F. and Duxbury P. M. (Editors), *Rigidity Theory and Applications* (Kluwer Academic, Plenum Publishers, New York) 1999.

[2] Smedskjaer M., Mauro J. C., Youngman R. E., Hogue C. L., Potuzak M. and Yue Y., *J. Phys. Chem. B*, **115** (2011) 12930.
[3] King S. *et al.*, *J. Non-Cryst. Solids*, **379** (2013) 67.
[4] Abdolhosseini Qomi M. J., Bauchy M., Pellenq R. and Ulm F. J., *Mechanics and Physics of Creep, Shrinkage, and Durability of Concrete*, edited by Ulm F. J., Hamlin J. and Pellenq R. (ASCE, Cambridge) 2013.
[5] Maxwell J. C., *Philos. Mag.*, **27** (1864) 294.
[6] Phillips J. C., *J. Non-Cryst. Solids*, **34** (1979) 155.
[7] Thorpe M. F., *J. Non-Cryst. Solids*, **57** (1983) 355.
[8] Feng X. W., Bresser W. J. and Boolchand P., *Phys. Rev. Lett.*, **78** (1997) 4422.
[9] He H. and Thorpe M. F., *Phys. Rev. Lett.*, **54** (1985) 2107.
[10] Micoulaut M. and Popescu M. (Editors), *Rigidity and Boolchand Intermediate Phases in Nanomaterials* (INOE Publishing House, Bucarest) 2009.
[11] Chubinsky M. V., Brire M.-A. and Mousseau N., *Phys. Rev. E*, **74** (2006) 016116.
[12] Jacobs D. J. and Thorpe M. F., *Phys. Rev. E*, **53** (1996) 3682.
[13] Ferlat G., Charpentier T., Seitsonen A. P., Takada A., Lazzeri M., Cormier L., Calas G. and Mauri F., *Phys. Rev. Lett.*, **101** (2008) 065504.
[14] Micoulaut M., Kerner R. and dos Santos-Loff D. M., *J. Phys.: Condens. Matter*, **7** (1995) 8035.
[15] Mauro J. C., Gupta P. K. and Loucks R. J., *J. Chem. Phys.*, **130** (2009) 234503.
[16] Bray P. J., Feller S. A., Jellison G. E. and Yun Y. H., *J. Non-Cryst. Solids*, **38-39** (1980) 93.
[17] Konijnendnik W. L. and Stevels J. M., *J. Non-Cryst. Solids*, **18** (1975) 307.
[18] Kamitsos E. I. and Chryssikos G. D., *J. Mol. Struct.*, **247** (1991) 1.
[19] Micoulaut M. and Phillips J. C., *Phys. Rev. B*, **67** (2003) 104204.
[20] Mosseri R. and Dixmier J., *J. Phys. Lett.*, **41** (1980) L5.
[21] Gupta P. K., *Proceedings of the XIV International Congress on Glass, New Delhi, India, 1986* (Indian Ceramic Society) 1986, p. 1.
[22] Selvenathan D., Bresser W. J. and Boolchand P., *Phys. Rev. B*, **61** (2000) 15061.
[23] Gunasekera K., Boolchand P. and Micoulaut M., *J. Appl. Phys.*, **115** (2014) 164905.
[24] Bril T. W., *Raman Spectroscopy of Crystalline and Vitreous Borates*, Thesis, Eindhoven University of Technology, May 1976, Phillips Research Report Suppl., 1976, No. 2.
[25] Galeener F. L., Lucovsky G. and Mikkelsen J. C. jr., *Phys. Rev. B*, **22** (1980) 3983.
[26] Lower N. P., McRae J. L., Feller H. A., Betzen A. R., Kapoor S., Affatigato M. and Feller A. S., *J. Non-Cryst. Solids*, **293-295** (2001) 669.
[27] Shelby J. E., *J. Am. Ceram. Soc.*, **66** (1983) 225.
[28] Novita D., Boolchand P., Malki M. and Micoulaut M., *Phys. Rev. Lett.*, **98** (2007) 195501.
[29] Micoulaut M. and Malki M., *Phys. Rev. Lett.*, **105** (2010) 235504.
[30] Micoulaut M., Malki M., Novita D. I. and Boolchand P., *Phys. Rev. B*, **80** (2009) 184205.
[31] Chen P., Holbrook C., Boolchand P., Georgiev D. G. and Micoulaut M., *Phys. Rev. B*, **78** (2008) 224208.
[32] Novita D. I., Boolchand P., Malki M. and Micoulaut M., *J. Phys.: Condens. Matter*, **21** (2009) 205106.
[33] Naumis G. G., *Phys. Rev.*, **83** (2011) 184204.
[34] Thorpe M. F., *J. Non-Cryst. Solids*, **182** (1995) 135.
[35] Micoulaut M. and Bauchy M., *Phys. Status Solidi B*, **250** (2013) 976.
[36] Smedskjaer M. M., Mauro J. C. and Yue Y., *Phys. Rev. Lett.*, **105** (2010) 115503.
[37] Mauro J. C. and Smedskjaer M., *Physica A*, **391** (2012) 6121.
[38] Sidebottom D. L. and Schnell S. E., *Phys. Rev. B*, **87** (2013) 054202.